Spatiotemporal Density Feature Analysis to Detect Liver Cancer from Abdominal CT Angiography

Yoshito Mekada[1], Yuki Wakida[2], Yuichiro Hayashi[2],
Ichiro Ide[2], and Hiroshi Murase[2]

[1] School of Life System Science and Technology, Chukyo University,
101 Tokodachi Kaizu Toyota, 470-0393, Japan
y-mekada@life.chukyo-u.ac.jp
http://www.st.chukyo-u.ac.jp/y-mekada/
[2] Graduate School of Information Science, Nagoya University,
Furo-cho, Chikusa-ku, Nagoya, 464-8603, Japan
yhayashi@suenaga.m.is.nagoya-u.ac.jp, ide@is.nagoya-u.ac.jp,
murase@is.nagoya-u.ac.jp

Abstract. In this paper, we propose a method of detecting liver cancers from dynamic X-ray computed tomography (CT) images based on a two-dimensional histogram analysis. In the diagnosis of a liver, a doctor examines dynamic CT images. These consist of four images, namely the pre-contrast phase, early phase, portal phase, and late phase ones, which are taken sequentially within a few minutes. Since the early and late phase images are important for diagnosing liver cancer, our method refers to both of them for detecting suspicious regions and eliminating false positives. First, it extracts liver cancer candidates by applying an adaptive neighbor type filter to the late phase image. Then, precise cancerous regions are specified by a region forming method. Most of the false positive regions are eliminated by two-dimensional histogram analysis of each region of interest. We applied the proposed method to 21 dynamic CT images. The results showed that sensitivity was 100% and there were 0.33 false positives per case on average.

1   Introduction

As a result of recent progress in computed tomography (CT) imaging devices such as multi-detector row CT(MDCT) scanners, these devices now generate a huge number of high-resolution slice images of a patient. In particular, in diagnosis using CT angiography, a doctor examines two or more three-dimensional images. For example in liver diagnosis, four CT images taken at different phases after the injection of a contrast medium are used routinely. Studying these images imposes a heavy load on medical doctors. Therefore, a computer aided diagnosis system is required.

In this paper, we propose a method of detecting liver cancer from CT angiography by using a registration technique and a two-dimensional histogram analysis of registered images. There has been some research on computerized

detection of cancerous regions from CT angiography [1-4]. Masumoto et al. [1] developed the image features for detecting cancer lesions from a single phase image, and Hong et al. [2] studied the same kind of scheme for three phase images independently. Watanabe et al. [3] proposed two kinds of density transition features to enhance the cancerous region. Their system needs four phase images that must be registered beforehand. Thus, their system suffers from the limitations of the medical situation. That is, in liver diagnosis, only the early and late phase images are frequently taken to reduce radiation exposure. Shimizu et al. [4] used the early and late phase images that were aligned using a non-rigid registration technique based on free-form deformation. They enhanced cancerous regions from each phase image independently by using an adaptive convergence index filter [5] and integrated these enhanced images into one image using addition operations. Some of these systems are sensitive to the image conditions and do not treat an important medical finding of hepatocellular carcinoma (HCC) mentioned in the next section.

The proposed system consists of three parts: detection of cancerous regions from late phase images, estimation of region borders, and false positive reduction based on two-dimensional histogram analysis to quantify important medical findings.

2 Characteristics of Liver Cancer

The early phase image is acquired shortly after the injection of contrast medium, and the late phase image is taken several minutes later. In a CT image, the contrast medium makes the CT value high because it absorbs more X-rays than the abdominal organs. In the early phase image, the contrast medium accumulates in the hepatic artery. It also accumulates in the HCC. On the other hand, in the late phase image, the contrast medium does not accumulate in any specific organ, but is distributed uniformly among all the organs. However, within an HCC lesion, the CT value is lower than that of surrounding tissues because the contrast medium had flowed out by that time.

Examples of each phase image are shown in Fig.1. From these figures, it looks easy to detect cancer regions from early phase images by using a simple thresholding technique. However, it is difficult to separate an HCC lesion from the hepatic artery because most HCCs are connected to the artery. On the other hand, in the late phase image, while differences in CT value between an HCC

(a) Pre-contrast phase   (b) Early phase   (c) Portal phase   (d) Late phase
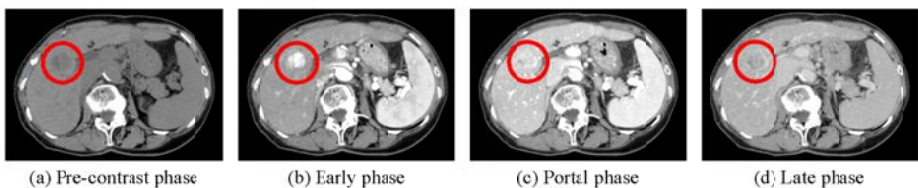
Fig. 1. Examples of CT angiogram

lesion and surrounding tissues are relatively small, the lesion border stands out clearly. Using these image features, we detect HCCs in the following way.

1. Partially detect a cancerous region from late phase images by spatial density analysis.
2. Estimate its border from late phase images by modifying the region forming method from partial borders.
3. Eliminate false positive regions by two-dimensional histogram analysis from early and late phase images aligned by a non-rigid registration technique.
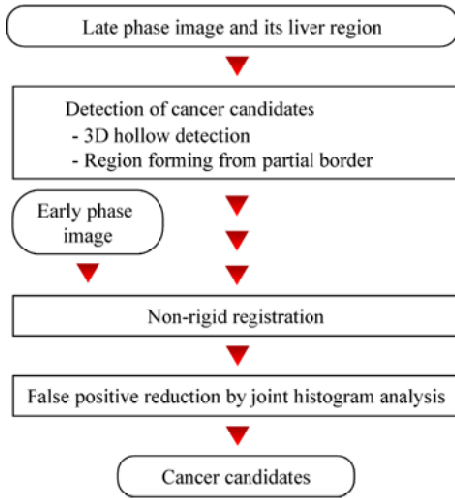
3   Method

The processing flow of our method is shown in Fig.2. The inputs are the early and late phase images and the liver region in the late phase image detected by the method given in ref. [6].

3.1   Detection of Cancer Candidates

We evaluated the features of cancer lesions in late phase images, where the CT value of a cancer lesion is lower than that of surrounding tissues. It is difficult to extract cancerous regions using a simple thresholding technique because there is no significant difference in CT value between a cancerous region and non-cancerous liver tissues. Therefore, we extracted hollows from the late phase image by applying an adaptive neighbor type filter. Then, precise cancerous regions were specified by a three-dimensional region forming method.

Finding Cancer Candidates. The adaptive neighbor type filter involves the following steps.

1. Set 26 search directions for an arbitrary voxel $\boldsymbol{x} = (i, j, k)$ in the liver region. The three components of direction vector $\boldsymbol{d}_n(|\boldsymbol{d}_n| > 0, n = 1, 2, \ldots, 26)$ are defined by all combinations of -1, 0, 1.
2. Find the nearest voxel that satisfies at least one of the following conditions for every n-th $(n = 1, 2, \ldots, 26)$ direction.
   (C1) $f(\boldsymbol{x} - r\boldsymbol{d}_n) - f(x) > T_1, r = (1, 2, \ldots, L_{max})$
   (C2) $h(\boldsymbol{x} - r\boldsymbol{d}_n) = 0, r = (1, 2, \ldots, L_{max})$,
   where $f(\boldsymbol{x})$ is the CT value at voxel $\boldsymbol{x}$ of the late phase images, h is a binary image whose value is 1 for the liver region detected by the method in [6] and 0 outside the liver region. L_{max} and T_1 are predefined threshold values. Only if the farthest voxel to $\boldsymbol{x}$ satisfying at least one above mentioned conditions is found in the n-th direction, we call this voxel a reach voxel R_n (see Fig.3).
3. Set the value of voxel $\boldsymbol{x}$ to 1 only if all the following three conditions are satisfied.
   (C3) Reach voxels are detected in all directions.
   (C4) The number of reach voxels located outside the liver region is smaller than a predefined threshold value T_2.

Fig. 2. Flow of the proposed method
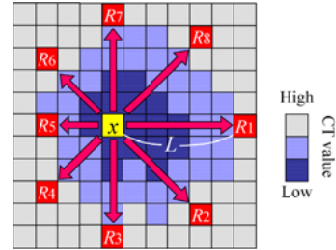
Fig. 3. Illustration of reach point

(C5) At least one reach voxel is located within the liver region from all combinations of two reach voxels that have point symmetry to voxel x.

The concept of this filter is similar to the Radial Reach Filter (RRF) proposed by Satoh et al. in [7]. The RRF is a two-dimensional robust gray value change detector for temporal subtracted images, while the filter that we propose is a three-dimensional hollow detector that is sensitive to changes in ambiguous gray values. Conditions (C2), (C4), and (C5) are taken into account to detect cancer lesions at the border of the liver for practical reasons.

Extraction of Precise Region of Cancer Candidates. In this section, we describe a technique for forming the three-dimensional border from partial border voxels. Using the above procedure, we can detect the central part of cancer lesions and some false positive regions. To eliminate these false positive regions by the histogram analysis (explained later), it is important to extract the precise cancerous region. However, it is difficult to detect the actual lesion border because of the unevenness of the contrast medium, unevenness of the cancer lesion itself, and the effect of the contacting tissues. Incidentally, reach voxels tend to be located close to the region border like the RRF [7]. The results of detected cancer candidates and the frequency image of reach voxels are shown in Fig.4. However, voxels that are frequently selected as cancer candidate voxels do not always form a closed surface if there are no significant differences at the partial lesion border. To cope with such situations, we extend the region forming method from the partial borders proposed by Sonka et al. [8] as follows.

1. Count the number of times that each voxel is selected as a reach voxel.
2. For all voxels x among cancer candidates, for all twenty-six directions, mark voxels located between x and the selected voxels as reach voxels most frequently.

3. Compute the number of times each voxel in the image is marked. Let $b(\boldsymbol{x})$ be the number of times voxel $\boldsymbol{x}$ is marked. If $\boldsymbol{x}$ is marked from a single direction, then $b(\boldsymbol{x})$ is set to zero.
4. The weighted number of marked $B(\boldsymbol{x})$ is determined as follows:

$$B(\boldsymbol{x}) = \begin{cases} 0 & for\ b(\boldsymbol{x}) = 0 \\ 1/27 & for\ b(\boldsymbol{x}) = 1 \\ 2/27 & for\ b(\boldsymbol{x}) = 2 \\ 5/27 & for\ b(\boldsymbol{x}) = 3 \\ 10/27 & for\ b(\boldsymbol{x}) > 3 \end{cases}$$

5. Compute $B_m(\boldsymbol{x})$ that is a median of $B(\boldsymbol{x})$ among the $3 \times 3 \times 3$ neighborhood of voxel $\boldsymbol{x}$.
6. Set the value of voxel $\boldsymbol{x}$ to one as a component of a cancer candidate if the sum of $B_m(\boldsymbol{x})$ of the $3 \times 3 \times 3$ neighborhood voxels is greater than 1.0, otherwise mark it as background.

Fig.5 shows the result of region forming method mentioned here.

(a)   (b)   (c)


(a)   (b)
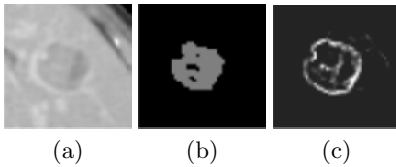
Fig. 4. Extracted cancer candidate and frequency image of reach voxels. (a) Magnified view of cancer lesion in late phase image. (b) extracted cancerous voxels by 3.1.1. (c) frequency image of reach voxels.
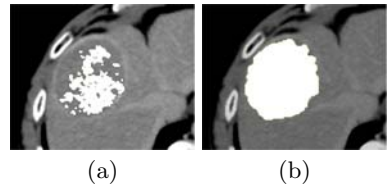
Fig. 5. Example of extracted cancer candidate after 3D region forming method. (a) extracted cancerous voxels by 3.1.1. (b) extracted results by region forming method.

4   Image Registration

The liver is an elastic organ, so it is easily deformed by the patient's respiration, and it also moves along with body movement. Since there is an interval of several minutes between the taking of early and late phase images of CT angiography, non-rigid registration is required for the evaluation of CT value transition. To align the early and late phase images, we used non-rigid registration using the free form deformation technique proposed by Rueckert et al. [9]. This non-rigid registration uses normalized mutual information as a similarity criterion. The early phase image is deformed based on the B-spline interpolation. Fig.6 shows examples of the integrated pre-registration of early and late phase images and the results of non-rigid registration of the two images. The chess-board visualization technique was used to show the results. Brighter rectangles correspond to the late phase image.

<center>(a)   (b)</center>
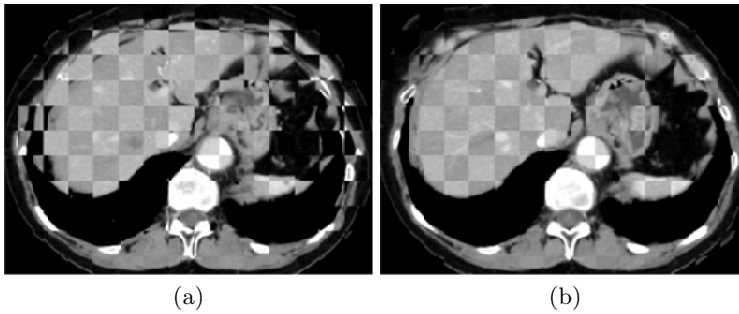
Fig. 6. The chess-board visualization of (a):pre-registration images and (b):the results of non-rigid registration

5   Elimination of False Positives

As mentioned in section 2, the CT value of the cancer lesion is higher than that of surrounding tissues in the early phase image and lower in the late phase image. False positive regions are eliminated by evaluating this phenomenon through the following procedure.

1. Definition of region of interest (ROI)
   The ROI is defined for each cancer candidate in order to include normal liver tissue around the cancer candidate region (CCR). The shape of the ROI is a rectangular parallelepiped, whose edges are parallel to the image axes. It is similar to the rectangular parallelepiped circumscribing each CCR. The ROI's center of gravity coincides with that of the CCR, and the volume of the ROI is determined to be 20 times that of the CCR. The volume of voxels outside the liver region is not taken into account in the ROI's volume.

2. Making a joint histogram of the ROI
   A joint CT value histogram of the ROI obtained using registered early and late phase images is calculated. This two-dimensional histogram has one large peak corresponding to the normal tissues around the CCR (see Fig. 7).

3. Estimation of normal tissue distribution
   In this step, the distribution of CT values of normal tissues around the CCR is estimated from the joint histogram. Most of the voxels in the ROI correspond to normal tissues. The joint histogram is projected onto each axis by the maximum intensity projection method. Then, the distribution of normal tissues is defined by the intersection of the following two closed intervals.

   $[\mu_x - 0.5\sigma_x, \mu_x + 0.5\sigma_x],$
   $[\mu_y - 0.5\sigma_y, \mu_y + 0.5\sigma_y],$

   where μ_x and σ_x are the average and standard deviation, respectively, of the curve projected onto the early phase axis, and μ_y and σ_y are those for the late phase axis.
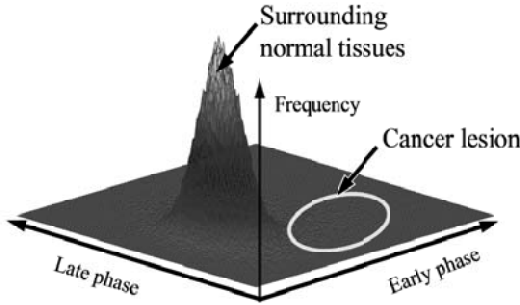
Fig. 7. Example of joint histogram

4. Estimation of the lesion's distribution
   Because the CT value of a cancer lesion is higher than that of normal tissues in the early phase image and lower in the late phase image, voxels satisfying both of the following conditions are detected as the cancerous region.
   - CT value of early phase is higher than $\mu_x + 0.5\sigma_x$
   - CT value of late phase is lower than $\mu_y - 0.5\sigma_y$
   Let H be the number of voxels in each CCR.
5. Elimination of false positives
   If H is small relative to the CCR volume, such a CCR might be a false positive region. Actually, all CCRs that satisfy the following condition are eliminated as false positives.
   $H/(S - C) \times 100 < T_3$,
   where S is the volume of CCR and C is the volume of cyst in the CCR. The CT value of the cyst is relatively low and hardly changes in the CT angiogram. In this experiment, voxels with a CT value lower than 50 [H.U.] were attributed to the cyst in the CCR.

6   Experiment

The procedure mentioned above was applied to 21 cases of multi-phase abdominal X-ray CT images. Every image was a slice with a size of 512×512 [points] having spatial resolution of about 0.6 [mm]. Nineteen cases were taken from a 4-line MDCT device and had a beam thickness of 2 [mm] and reconstruction interval of 1 [mm]. The other two cases were taken from a 16-line MDCT device

Table 1. Image specification of CT images

|	
Image size	512×512
# of slices	$161\sim464$
Pixel size[mm]	$0.546\sim0.625$
Reconstruction pitch[mm]	$0.5\sim1.0$
Slice thickness[mm]	$1.0\sim2.0$

and had a beam thickness of 1 [mm] and reconstruction interval of 0.5 [mm]. Seventeen cases included one or more liver cell cancers and the other four cases had no cancer lesions. The image specifications are shown in Table 1. Threshold values were set to $T_1 = 15, T_2 = 13$, and $T_3 = 16$, experimentally.

7   Results

The experimental results show that the average number of false positives per case was 0.33 with sensitivity of 100%. This result is promising because it shows fewer false positives per case for the same database than refs. [3] and [4], which had 0.71 and 0.53, respectively. Fig. 8 shows a free-response receiver operating characteristic(FROC) curve drawn by changing the threshold value T3. Some detection results are shown in Fig. 9 and 10. False positives that still remained were located at the border of the liver. The cancer lesion corresponding to the minimum value of the false positive elimination criterion makes it difficult to improve accuracy. In this experiment, extraction of the precise border did not work well because this lesion was surrounded by many cysts.
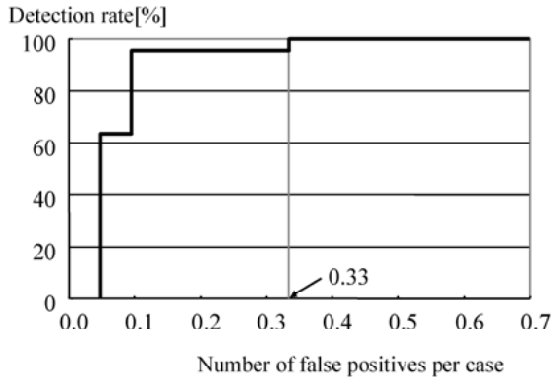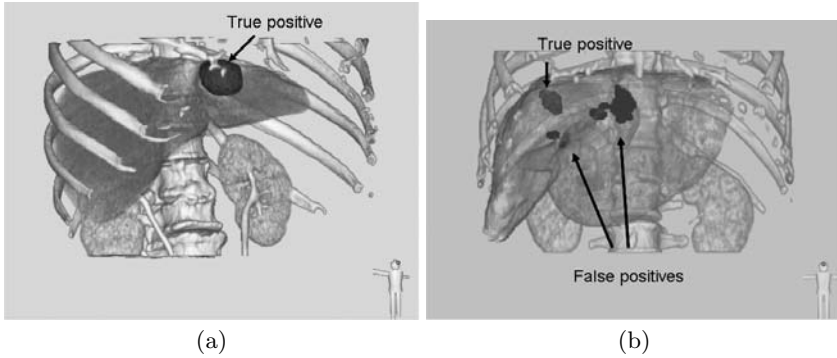

Fig. 8. The FROC curve drawn by changing the threshold value T_3

| (a) | (b) | (c) | (d) |
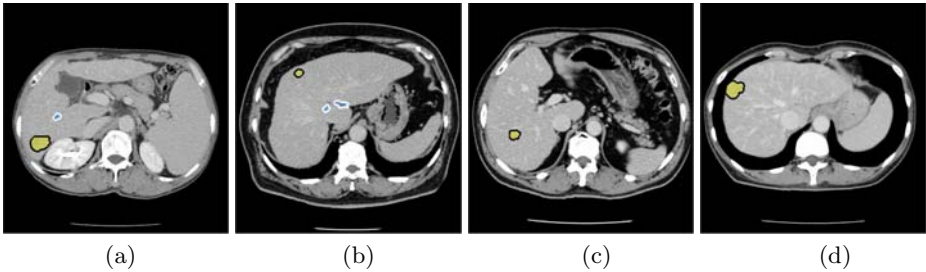
Fig. 9. Examples of detection results. Regions surrounded by the black line are the cancer lesions detected correctly. Regions surrounded by the white line are false positives eliminated correctly.

(a)   (b)

Fig. 10. Volume rendering views of results. Yellow regions are the cancer lesions detected correctly. Blue regions are false positives eliminated correctly.

8   Conclusion

This paper presented a novel computer aided liver cancer detection system for three-dimensional CT angiogram. The concept consists of the following.

– Integration of the early and late phase images by non-rigid registration
– Quantification of the density transition state, which is an important diagnostic finding, for each cancerous region detected by spatial density analysis

First, spatial density analysis is used to detect ambiguous three-dimensional hollows as cancer candidates and form a precise region from partial border voxels. Then, spatiotemporal density feature analysis of the two aligned images (early and late phase images) is performed to eliminate false positives. Experimental results showed that the number of false positive regions per case was 0.33 with sensitivity of 100%. This is superior to previous work using the same image database [3, 4]. In the future, we plan to perform fine registration for each ROI to eliminate false positives and develop some new features to reduce false positives.

References

1. J. Masumoto M. Hori, Y. Sato, T. Murakami, T. Johkoh, H. Nakamura and S. Tamura, "Automated detection of liver tumors in X-ray CT images", IEICE Trans. J83-D, No.1, pp.219–227, 2000.(in Japanese)
2. J. Hong, T. Kaneko, R. Sekiguchi, Kh. Park, "Automatic liver tumor detection from CT", IEICE Trans. Inf. Syst. E84-D No.6, pp.741–748, 2001.

3. S. Watanabe, Y. Mekada, J. Hasegawa and J. Toriwaki,"Liver cancer detection by using transition features obtained from multi-phase CT image", Proceedings of SPIE, Vol.5747, pp.783–789, 2005.
4. A. Simizu, T. Kawamura and H. Kobatake, "Proposal of computer-aided detection system for three dimensional CT images of liver cancer", Proc. of Computer Assisted Radiology and Surgery (CARS2005) 19th International Congress and Exhibition, International Congress Series 1281, pp.1157–1162, 2005.
5. H. Kobatake, W. Jun, Y. Yoshinaga, Y. Hagihara and A. Shimizu , "Nonlinear adaptive convergence index filter and their characteristics", Proc. of ICPR2000, Vol.3, pp.526–529, 2000.
6. Y. Hayashi, D. Deguchi, K. Mori, Y. Mekada, Y. Suenaga and J. Toriwaki, "Development of a method for automated liver region extraction from contrasted 3D abdominal X-ray CT images", Journal of Computer Aided Diagnosis of Medical Images, Vol.8, No. 1‑3, pp.18–30, 2004.(in Japanese)
7. Y. Satoh, H. Tanahashi, C. Wang, S. Kaneko, Y. Niwa, K. Yamamoto, "Robust Event Detection by Radial Reach Filter", Proc. of 16th ICPR, Vol.2, pp623–626, 2002.
8. M. Sonka, V. Hlavac, R. Boyle, "Image Processing, Analysis, and Machine Vision", PWS Publishing, pp.174–176, 1998.
9. D. Rueckert, L. I. Sonoda, C. Hayes, D. L. G. Hill, M. O. Leach, and D. J. Hawkes, "Nonrigid Registration Using Free-Form Deformations: Application to Breast MR Images", IEEE Trans. Medical Imaging, Vol.18, No.8, pp.712–721, 1999.